Supporting Information

Doping Lanthanide into Perovskite Nanocrystals: Highly Improved and Expanded Optical Properties

Gencai Pan,[†] Xue Bai,[†] Dongwen Yang,[‡] Xu Chen,[†] Pengtao Jing,[§] Songnan Qu,[§] Lijun Zhang,[‡] Donglei Zhou,[†] Jinyang Zhu,[†] Wen Xu,[†] Biao Dong,[†] and Hongwei Song[*†]*

[†]State Key Laboratory on Integrated Optoelectronics, College of Electronic Science and Engineering and [‡]*Key Laboratory of Automobile Materials of MOE, State Key Laboratory of Superhard Materials, and College of Materials Science and Engineering, Jilin University, Changchun 130012, China*

[§]State Key Laboratory of Luminescence and Applications, Changchun Institute of Optics Fine Mechanics and Physics Chinese Academy of Sciences, Changchun 130033, China

[*]E-mail: baix@jlu.edu.cn

[*]E-mail: songhw@jlu.edu.cn

Methods

Materials. Cs_2CO_3 (99.9%), octadecene (ODE, 90%), oleic acid (OA, 90%) oleylamine (OLA, 70%), $PbCl_2$ (99.99%), $CeCl_3•6H_2O$ (99.99%), $SmCl_3•6H_2O$ (99.99%), $EuCl_3•6H_2O$ (99.9%), $TbCl_3•6H_2O$ (99.9%), $DyCl_3•6H_2O$ (99.9%), $ErCl_3•6H_2O$ (99.9%), $YbCl_3•6H_2O$ (99.9%)，toluene (ACS grade, Fischer), ODE was purchased from Macklin, others were purchased from Sigma-Aldrich and all were used directly.

Synthesis of $CsPbCl_3$ perovskite NCs. $PbCl_2$ (0.105 g), OAm (1 mL), OA (1 mL), and ODE (10 mL) were added to a 50-mL 3-neck round-bottom flask and were stirred and refilled with N_2 followed by heating the solution to 120 °C for 1 hour. The solution was then increased to 180 °C and maintained for 10 minutes. Then the required temperature increased, the Cs-oleate (0.8 mL) was swiftly injected and after 30 s the solution was cooled with an ice bath. The NCs were precipitated with acetone and the centrifuged followed by dissolution in toluene.

Synthesis of lanthanide ions doped $CsPbCl_3$ perovskite NCs. Lanthanide-doped $CsPbCl_3$ perovskite NCs were prepared by hot injection method as reported previously with some modification. Firstly, lanthanide chloride (0.188mmol) was adequately dissolved into 10 ml octadecene (ODE) at 160 °C for 1 h under purging N_2 gas. Next, lead chloride (0.376 mmol) was added and continued heated at 160 °C for 1 h. After the complete dissolution of lanthanide and lead chlorides, the temperature was raised to 240 °C under purging N_2 gas. The as-prepared Cs-oleate was then injected into the contents promptly, and after 30 s, the flask was immediately placed in an ice-water bath to stop the particle growth. The lanthanide ions doped perovskite NCs in the ODE were centrifuged at 5000 rpm for 10 min and the supernatant was discarded. The precipitate was dispersed in toluene, and then centrifuged again at 12000 rpm for 10 min. The resultant NCs were re-dispersed in toluene for a second time. After resting 1 day, the supernatant was required colloidal lanthanide ions doped perovskite NCs. Four doping concentrations (1.2 mol%、2.7 mol%、7.8 mol% and 11.1 mol%) of Eu^{3+}

ions were gotten by four corresponding hot injection temperatures (180 °C , 200 °C , 240 °C and 260 °C).

Synthesis of Ce^{3+} and Eu^{3+} co-doped $CsPbCl_3$ NCs. Firstly, (0.06mmol) $CeCl_3$ and (0.188mmol) $EuCl_3$ was adequately dissolved into 10 ml octadecene (ODE) at 160 °C for 1 h under purging N_2 gas. Next, the lead chloride (0.376mmol) was added and continued for 1 h. After complete dissolution of lanthanide and lead chloride, the temperature was raised to 240 °C under purging N_2 gas. The as-prepared Cs-oleate was then injected into the contents promptly, after 30 s, which was immediately transferred to an ice-water bath. After centrifugation, the supernatant was discarded and the precipitates were re-dispersed in toluene, forming a stable colloidal solution.

Characterizations. Powder XRD patterns were recorded by using a Rigaku D/Max-Ra X-ray diffractometer with a monochrom at Cu Kα radiation (λ = 1.54178 Å). For TEM measurements, a Titan transmission electron microscope (FEI Company) operated at 300 kV was used. For the HRTEM measurements, the samples were imaged in EFTEM mode with a 20 KeV energy slit inserted around the zero energy loss of electrons. Trace Metal Analysis was carried out using inductively coupled plasma optical emission spectrometry (ICP-OES) on a Varian 720-ES ICP-optical emission spectrometer. X-ray photoelectron spectroscopy (XPS) was carried out in a Kratos Axis Ultra DLD spectrometer equipped with a monochromatic Al K_α X-ray source (hν = 1486.6 eV) operated at 150 W with a multichannel plate, and a delay line detector under 1.0×10^{-9} Torr vacuum.

DFT Calculations. All first principle calculations are carried out by using plane-wave pseudopotential methods within density functional theory (DFT) as implemented in the Vienna Ab-initio Simulation Package (VASP).[1-4] The electronic wave-functions are expanded in plane-wave basis sets with kinetic energy cutoff of 300 eV. The electron-ion interactions are described with the projected augmented wave (PAW) pseudopotential[5] and electron configurations of $5s^25p^66s$ for Cs,$6s^25p^2$ for Pb, $3s^23p^5$ for Cl and $5s^25p^65d^16s^2$ for La are considered as valence electrons. The defect

formation energies are given by: $\Delta H = (\mathrm{E}_D - \mathrm{E}_0) - \sum_i n_i(\mu_i + \mu_i^{bulk}) + q(\varepsilon_{VBM} + \varepsilon_f)$

where E_D and E_h are the total energies of the defect-containing and the host (i.e. defect-free). μ_i is the relative chemical potential for the i'th atomic species, referenced to its bulk μ_i^{ref} .ε_{VBM} is the energy of the VBM and ε_f is the Fermi energy relative to the host VBM.The transition level of a defect, $\varepsilon(q/q')$, corresponding to a change in its charge state between q and q', is given by the Fermi level, at which the formation energies, ΔH (q) and ΔH (q'), for charge states q and q' are equal to each other:

$$\varepsilon(q/q') = [\Delta H(q) - \Delta H(q')]/(q' - q)$$

The defect formation energies are calculated using PBE function with the VBM and CBM from PBE calculation corrected using the G_0W_0 calculations.[6] Corrections to the defect formation energies due to potential alignment, band filling effects, and image charge corrections are applied wherever appropriate.[7] The experimental lattice constants are used in all calculations. We used a 3×3×3 supercell (135 atoms if defect free) with the Γ point for the defect formation energies and transition levels.

Optical studies. UV−Vis absorption spectra were obtained by using a Shimadzu UV-3101PC scanning spectrophotometer. The samples were pumped using a laser-system consisting of a Nd: YAG pumping laser (1064 nm), a third-order Harmonic-Generator (355 nm) and a tunable optical parameter oscillator (OPO, Continuum Precision II 8000) with a pulse duration of 10 ns, a repetition frequency of 10 Hz and a line width of 4-7 cm^{-1}. A visible photomultiplier (350-850nm) combined with a double-grating monochromator were used for spectral collection. The PL QYs of the samples were acquired using an integrating sphere incorporated into a spectrofluorometer (FLS980, Edinburgh Instruments). Quantum yield was then calculated by using the Edinburgh L980 software package.

Femto-second transient absorption spectra were collected using an ultrafast system Helios spectrometer with broadband capability and time resolution of 120 fs. The probe pulse was generated in a 2 mm thick calcium floride (CaF_2) plate in the Helios spectrometer using a few microjoules of pulse energy from the fundamental output of

a Ti:sapphire femtosecond regenerative amplifier operating at 800 nm with 35 fs pulses and a repetition rate of 1kHz. The pump pulses at 365 nm were created from spectrally tunable (240−2600 nm) femtosecond pulses generated in the optical parametric amplifier (Newport Spectra-Physics). The transmitted probe light from the samples was collected and focused on the broadband UV−visible detector to record the time-resolved transient absorption spectra.

LED Fabrication. The powder of $CsPbCl_3$: Ce^{3+} (2%): Eu^{3+} (8%) NC is mixed Polymethylmethacrylate (PMMA) in toluene, and put ted in a vacuum chamber and stirred for 2h, at last, the viscous mixture was coated on a commercially available 365nm GaN LED chip, and putted the as-prepared LEDs in fume cupboard for 10 hours. After drying of the color conversion layer, the LEDs from Ce^{3+} and Eu^{3+} ions co-doped $CsPbCl_3$ NCs were fabricated.

Material Stability. The photo-stability measurement of the material is achieved under UV light illumination. And the PL intensity of undoped and 7.8 mol% Eu^{3+} doped $CsPbCl_3$ NCs was detected for 36h.

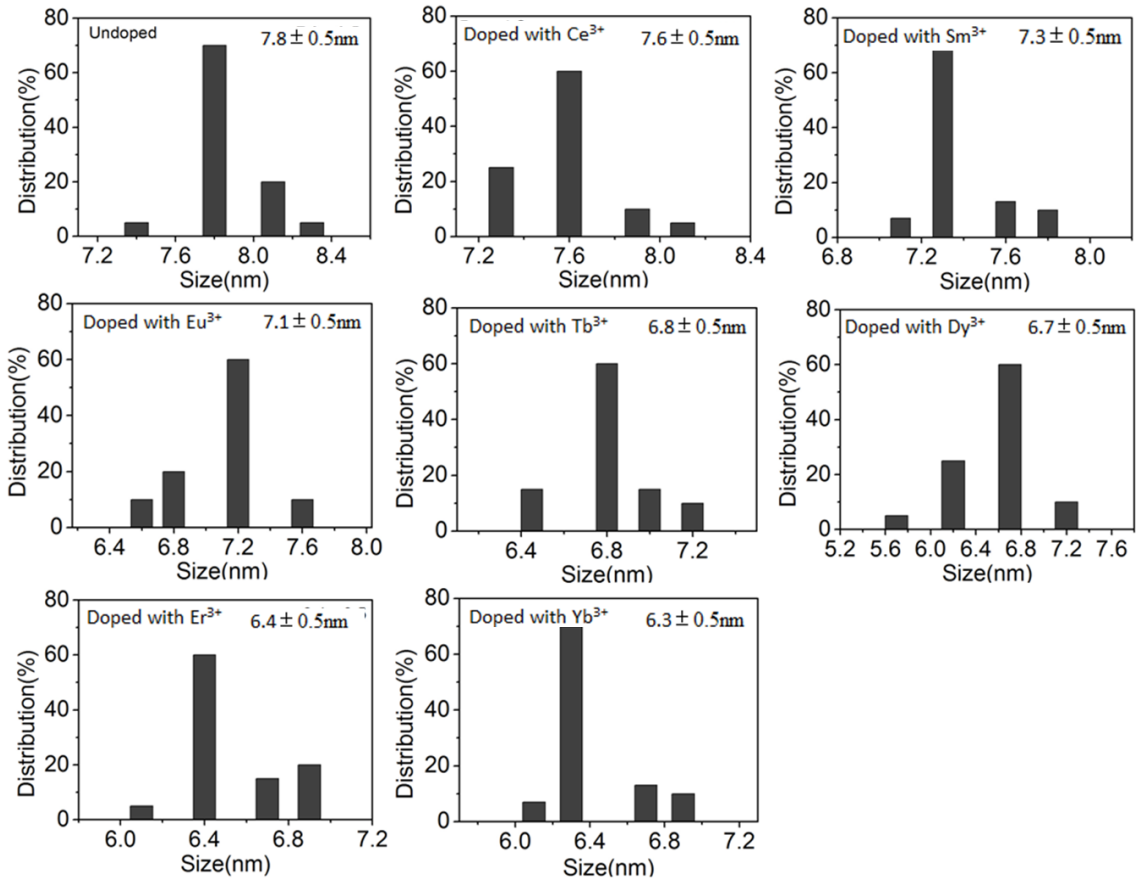

Figure S1. Particle size distribution plots of the undoped and lanthanide ions doped $CsPbCl_3$ NCs calculated from TEM images.

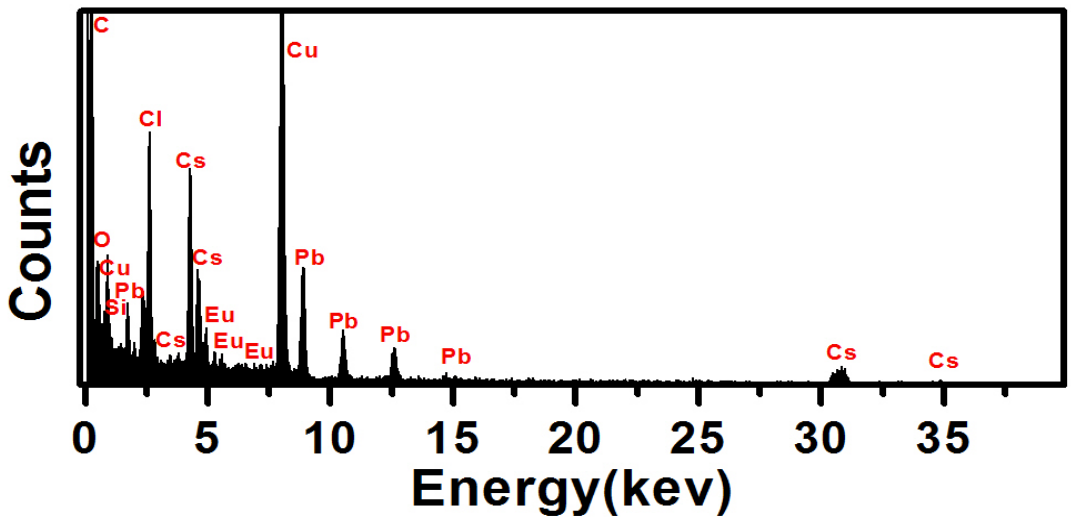

Figure S2. EDX pattern of Eu^{3+} ions doped $CsPbCl_3$ NCs prepared at the injection temperature of 240 °C.

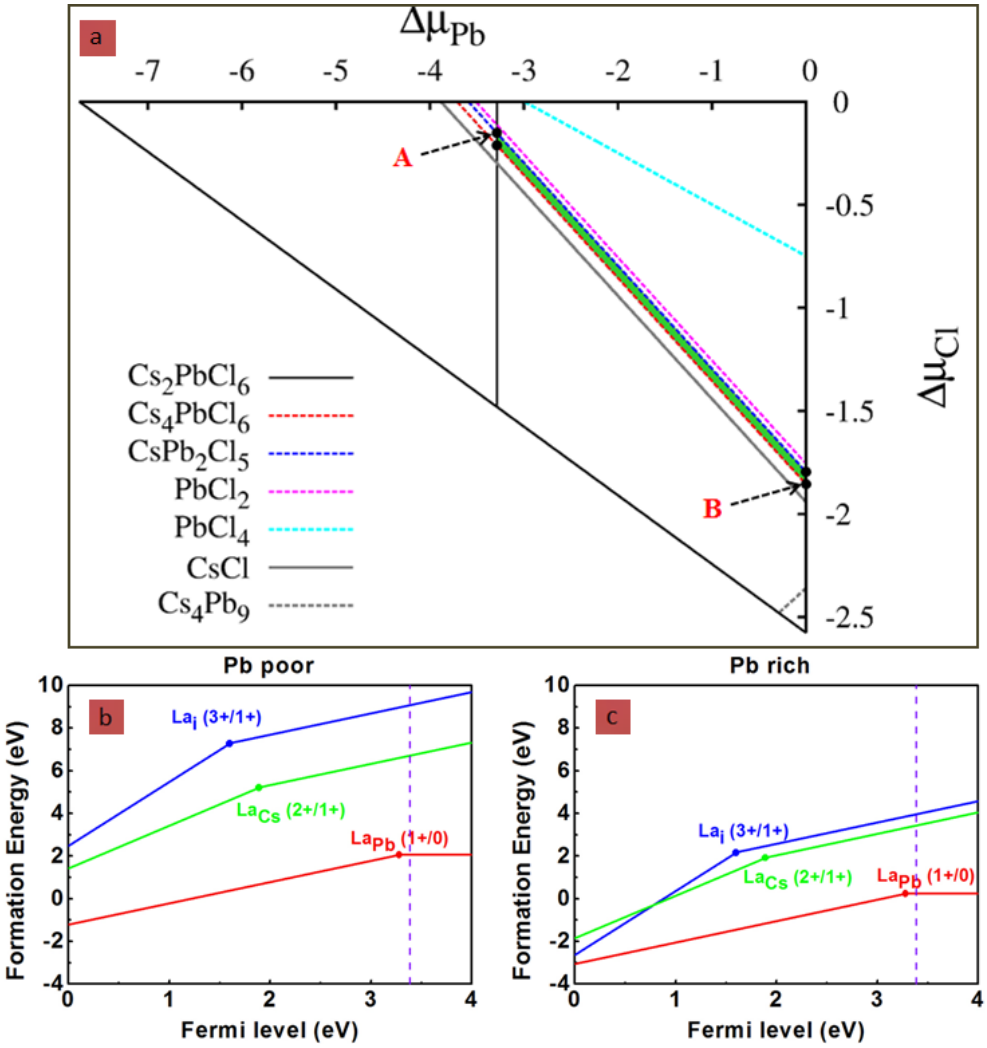

Figure S3. (a) Phase stability diagram analysis results at varied growth conditions represented by $\Delta\mu_{Pb}$ and $\Delta\mu_{Cl}$ for $CsPbCl_3$. The polygon region in green represents thermodynamic stable condition and each dash line corresponds to one competing phase of ternary compound $CsPbCl_3$. Point A and point B refer to the Pb-poor and Pb-rich conditions, respectively. **(b)** and **(c)** Calculated formation energies (ΔH) of La_{Pb}, La_i and La_{Cs} as a function of Fermi level using chemical potentials corresponding to points A and B in (a). Slopes of the formation energy lines indicate the charge states of the defects. A transition level is where the slope changes.

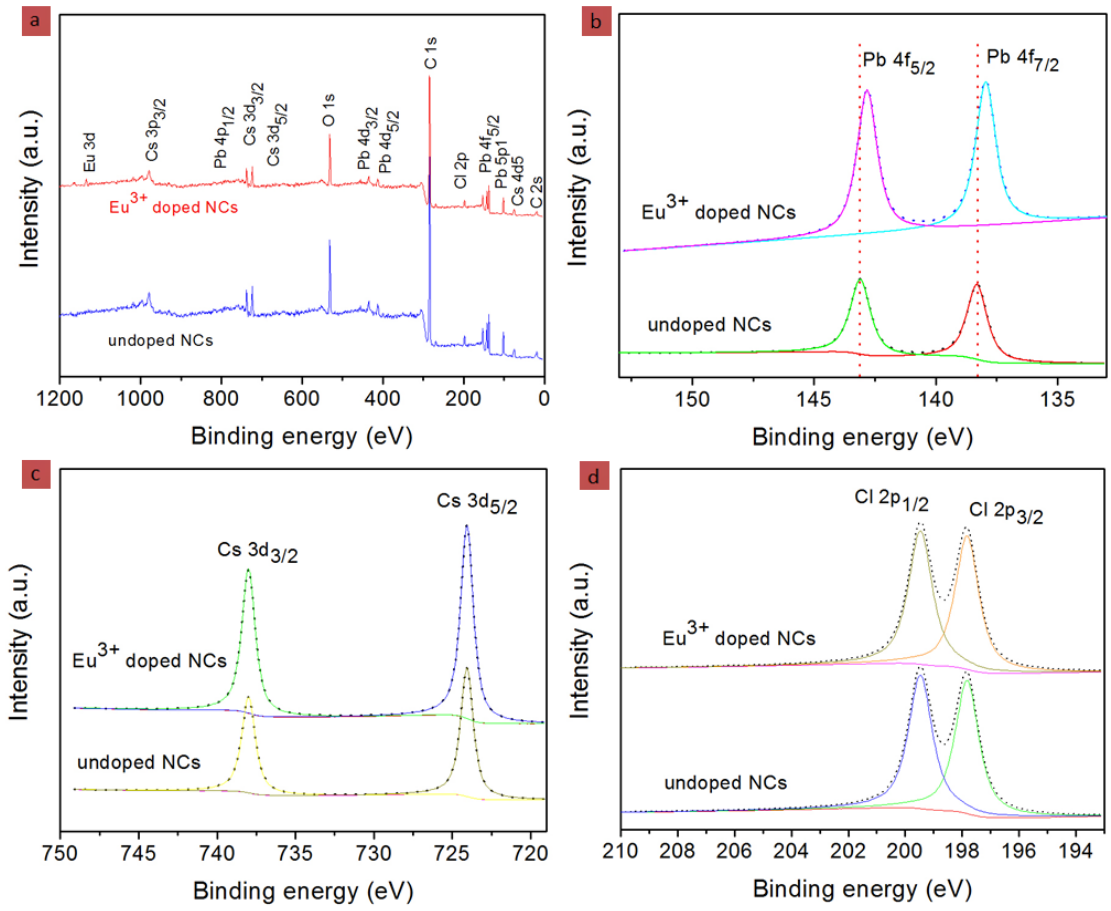

Figure S4. (a) Survey XPS spectrum for the undoped and 7.8 mol% Eu^{3+} ions doped $CsPbCl_3$ perovskite NCs, **(b, c** and **d)** the high-resolution XPS analysis corresponding to Pb^{2+} 4f, Cs^{+} 3d, and Cl^{-} 2p, respectively.

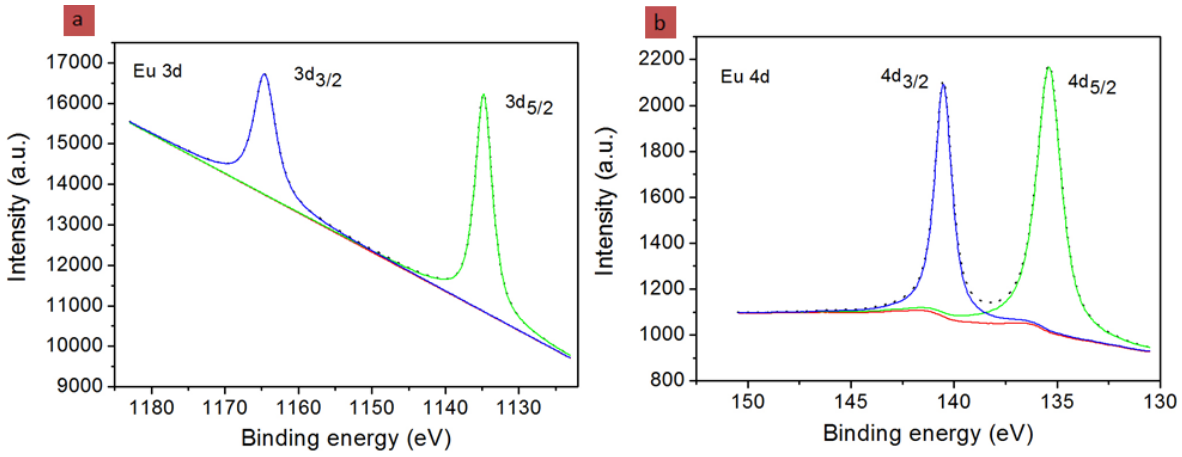

Figure S5. High-resolution XPS analysis corresponding to **(a)** Eu $3d_{3/2}$ and **(b)** Eu $4d_{3/2}$ for the Eu^{3+} ions doped $CsPbCl_3$ NCs.

The binding energy of Eu^{3+} 3d suggests some $EuCl_3$ adsorbed on the surface of NCs, while the binding energy of Eu^{3+} 4d suggests the Eu^{3+} ions were doped into the lattice of NCs.

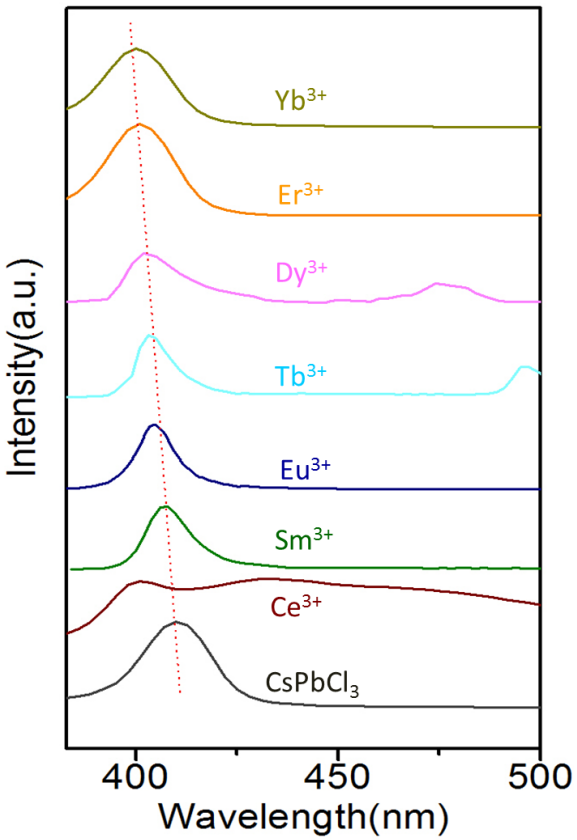

Figure S6. Emission spectra of $CsPbCl_3$ NCs doped with different lanthanide ions. The emissions are associated to the exciton transition of $CsPbCl_3$ NC host and the spectra are translated along the vertical axis to render easier the comparison between them.

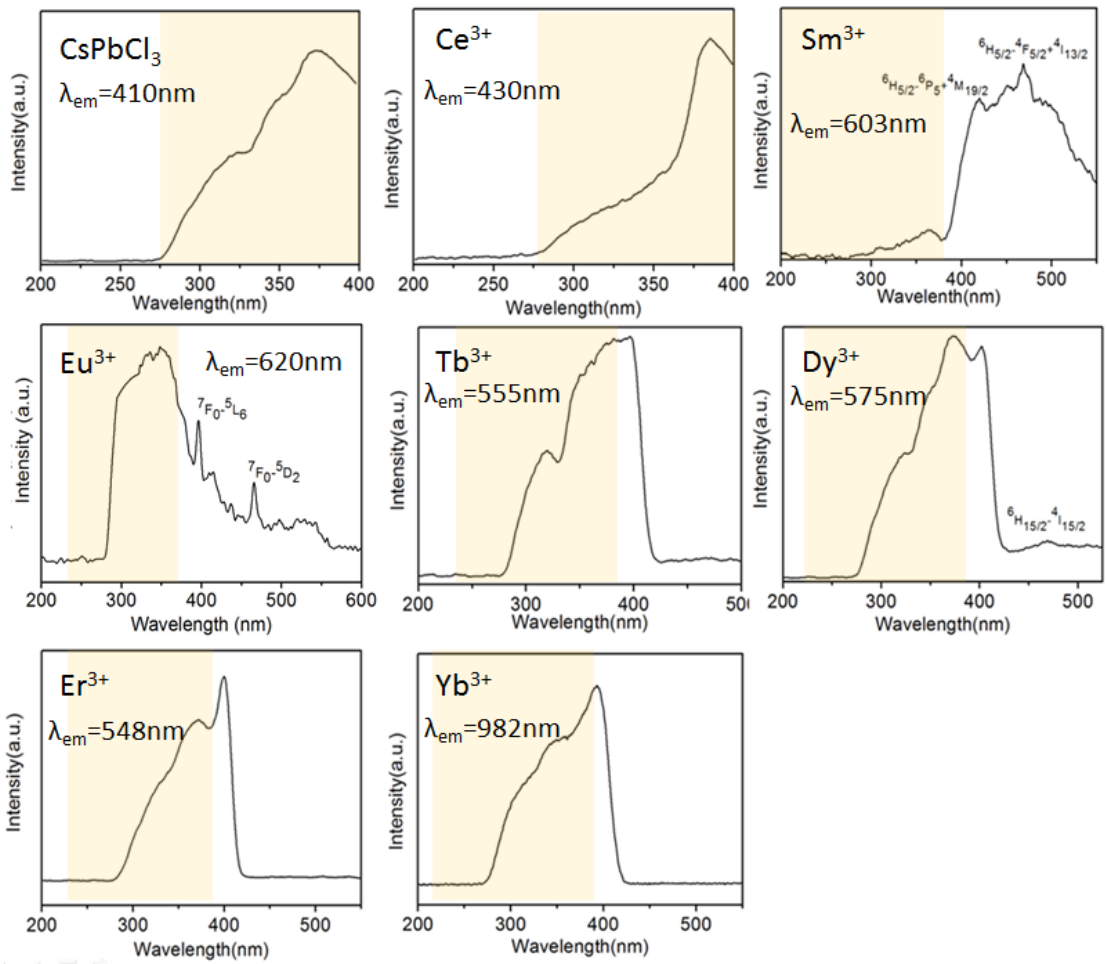

Figure S7. The excitation spectra of $CsPbCl_3$ NCs doped with different lanthanide ions recorded by monitoring at the respective intrinsic emissions of lanthanide ions.

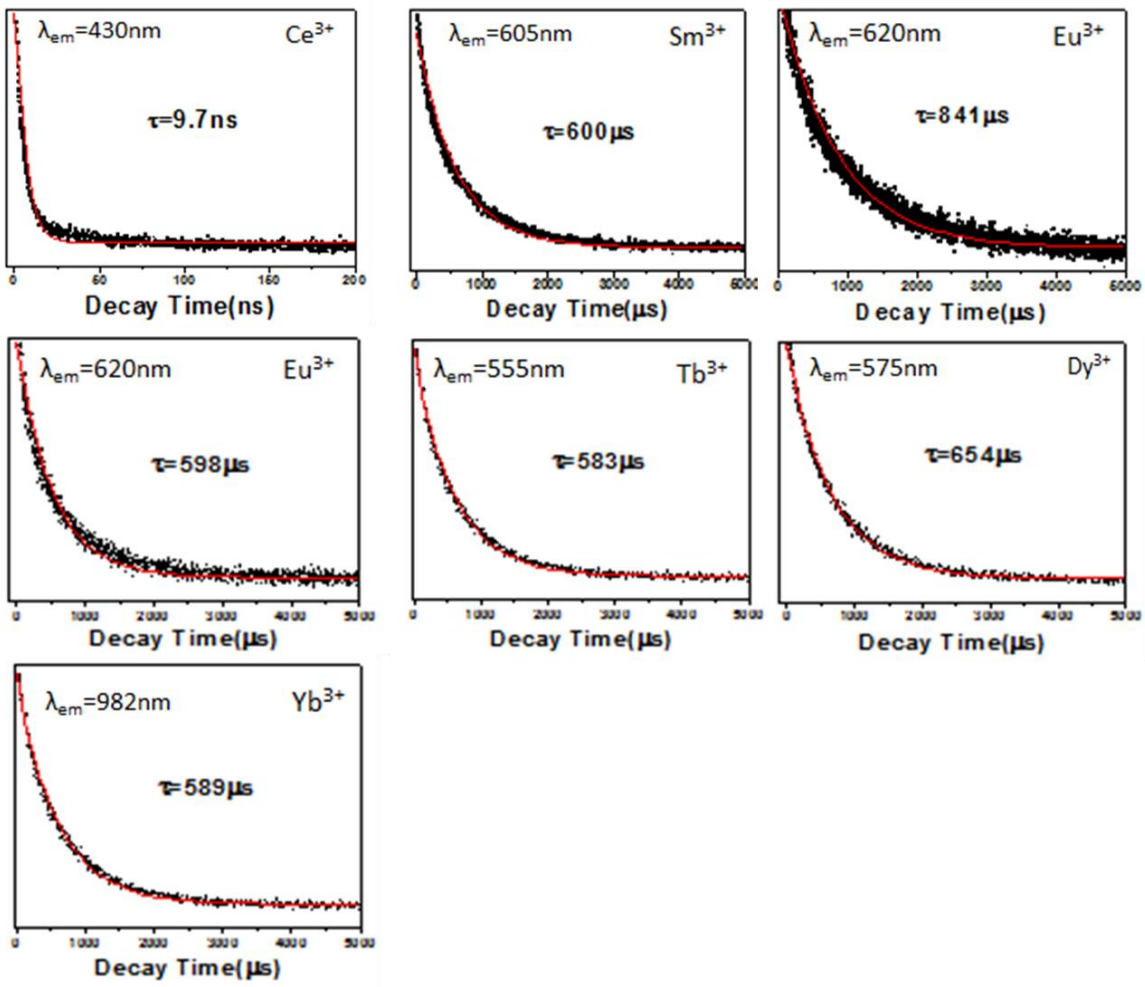

Figure S8. Emission decays for the $CsPbCl_3$ NCs doped with different lanthanide ions acquired by monitoring the respective intrinsic transitions of the lanthanide ions.

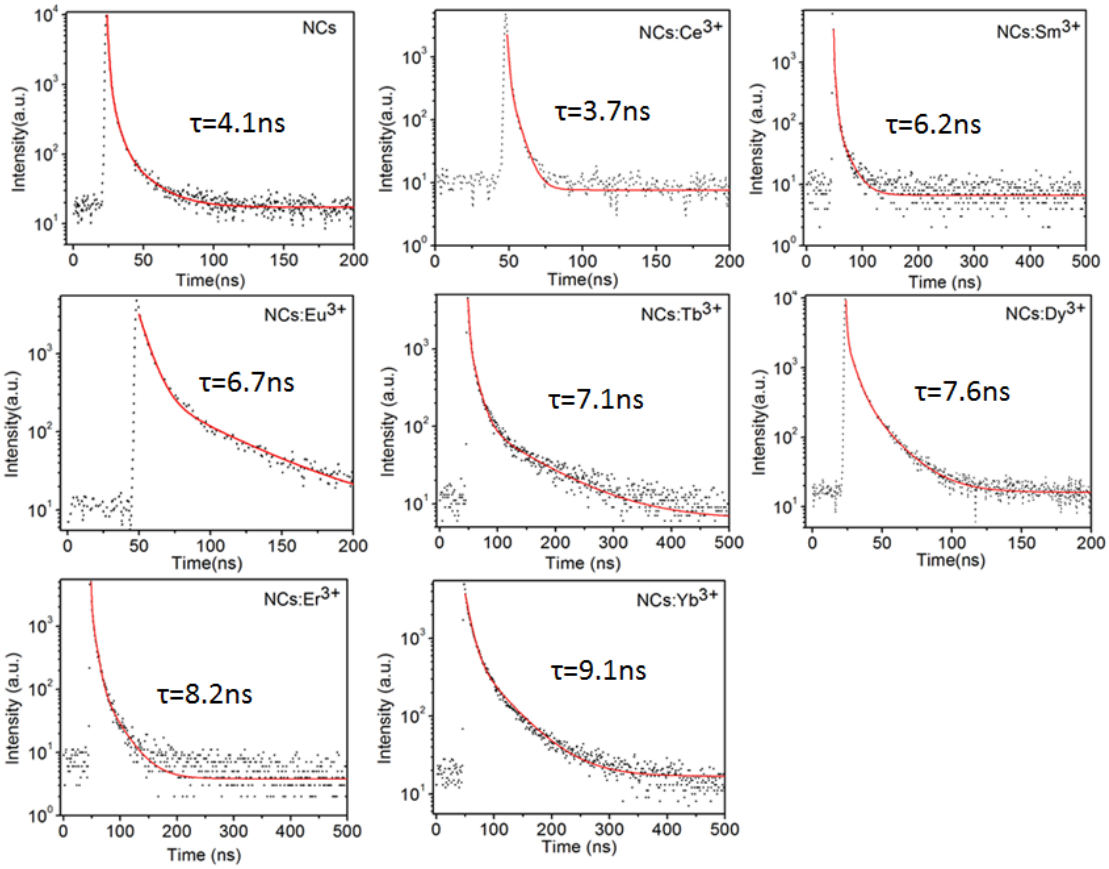

Figure S9. Emission decays of excitonic transitions (monitored at 410 nm) for the undoped $CsPbCl_3$ NCs and NCs doped with different lanthanide ions.

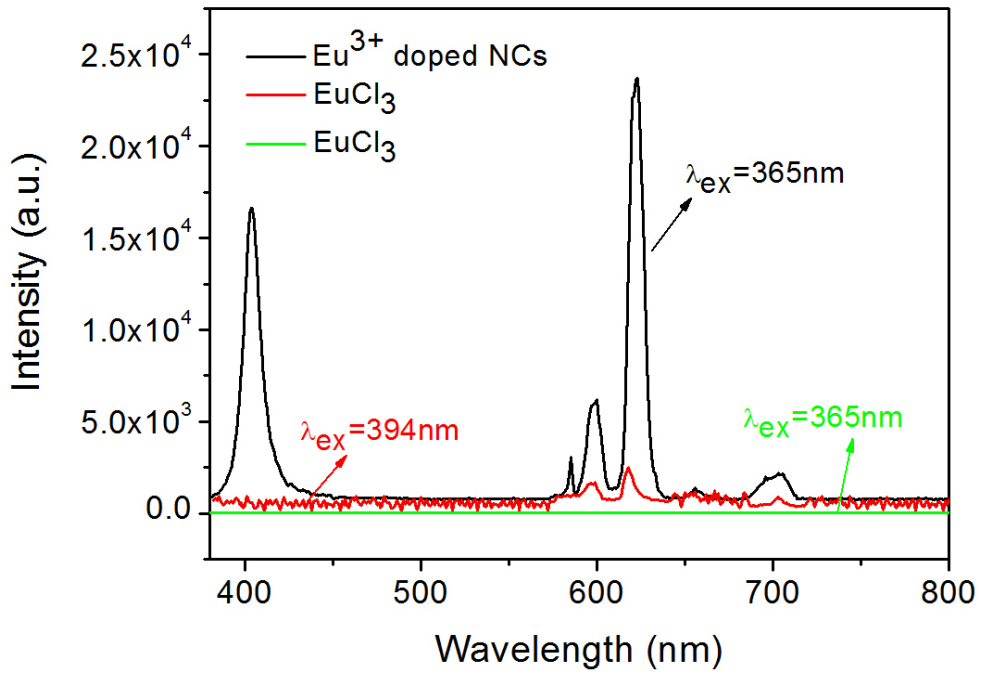

Figure S10. Emission spectra of Eu^{3+} doped $CsPbCl_3$ NCs and $EuCl_3$ (purchased from Macklin) in toluene. The intensity of emission spectrum of $EuCl_3$ was magnified by 100 times (red line).

The $EuCl_3$ in toluene has no detectible photoluminescence under the excitation of 365 nm (green line). Under the intrinsic excitation of Eu^{3+} ions (394 nm), the $EuCl_3$ toluene solution present extremely low $^5D_0$-^7F_J (J=0,1,2) emissions (red line), which is three-order lower than the present photoluminescence of Eu^{3+} ions doped $CsPbCl_3$ NCs.

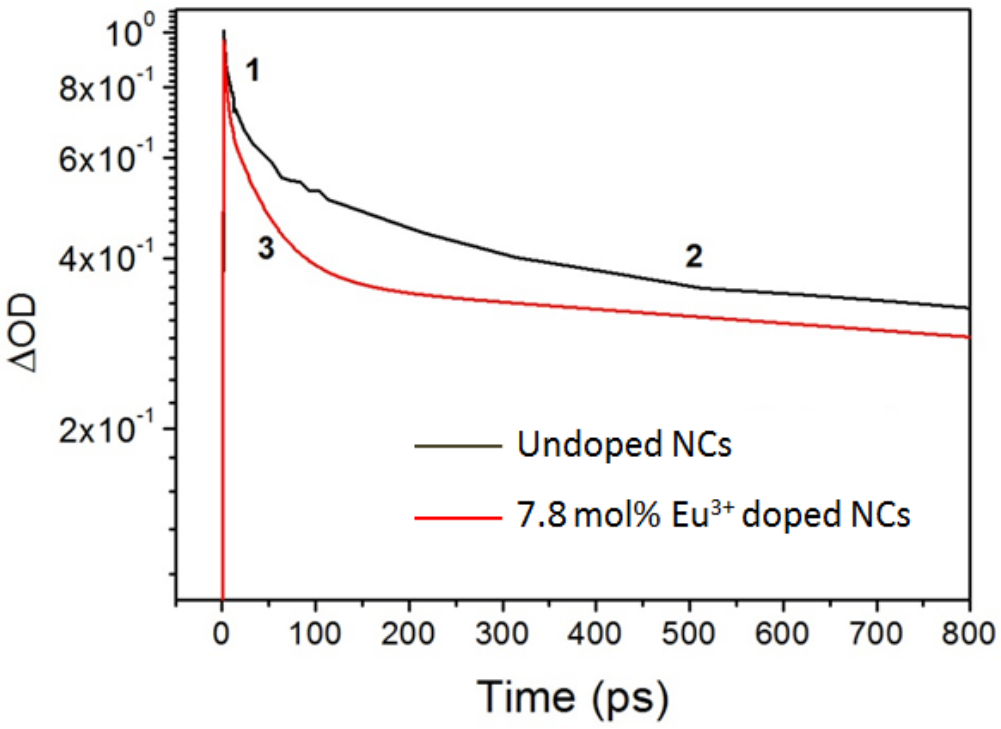

Figure S11. The typical fs-transient kinetics traces of undoped and Eu^{3+} ions doped $CsPbCl_3$ NCs monitored at the respective GSB maxima.

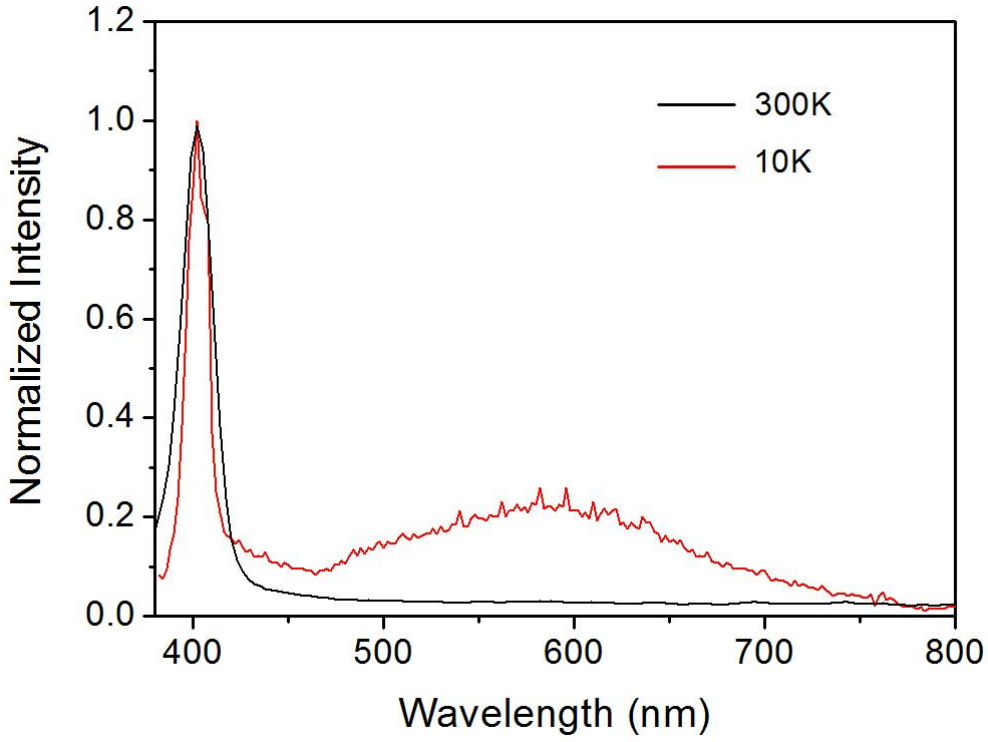

Figure S12. The emission spectra for the Yb^{3+} ions doped $CsPbCl_3$ perovskite NCs under excitation of 365 nm at 10 K and 300 K.

As shown in the Figure S12, the emission spectrum for the Yb^{3+} ions doped CsPbCl3 perovskite NCs presents an additional broad component (full-width-at-half-maximum, FWHM, *ca.* 120 nm) centered at around 596 nm comparing with the spectra acquired at room-temperature. This new component is consistent with the emission from some defect state in the NCs, indicating that there are some intermediate energy levels existed between the valence and conduction band of perovskite NC host.

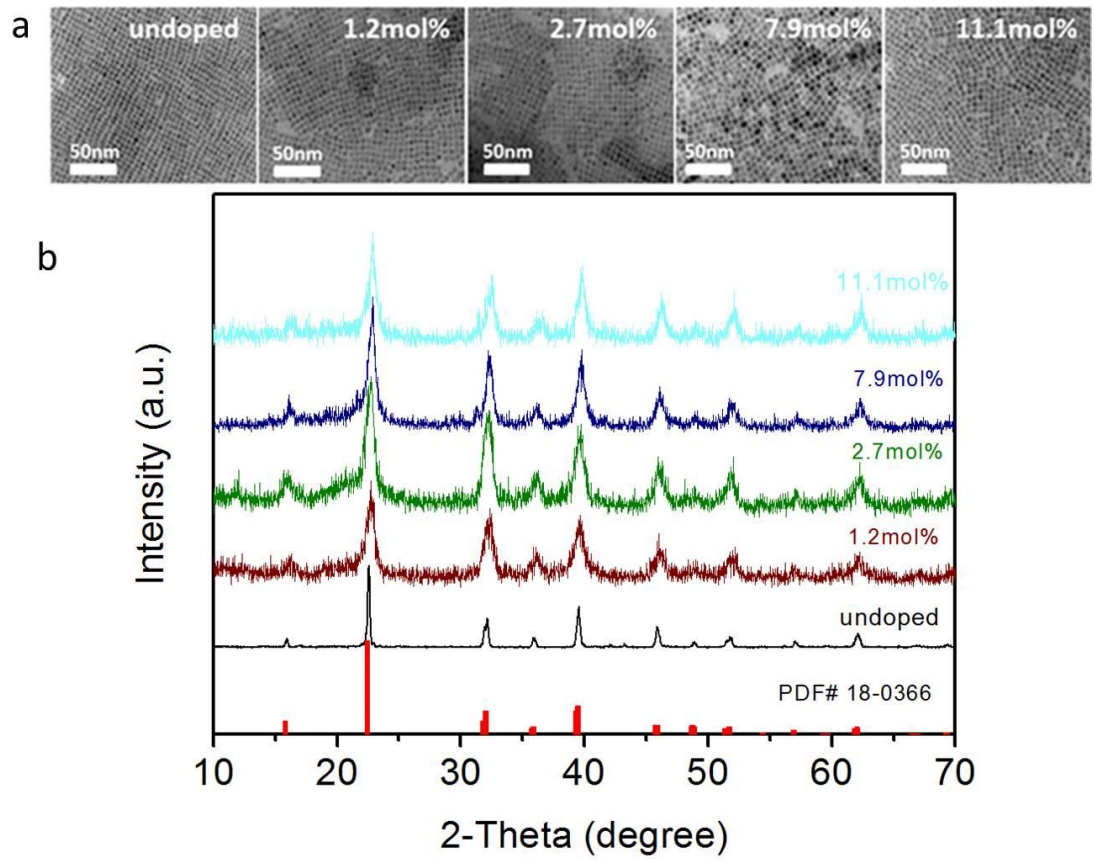

Figure S13. TEM images and XRD patterns of $CsPbCl_3$ NCs doped with different Eu^{3+} ion concentrations.

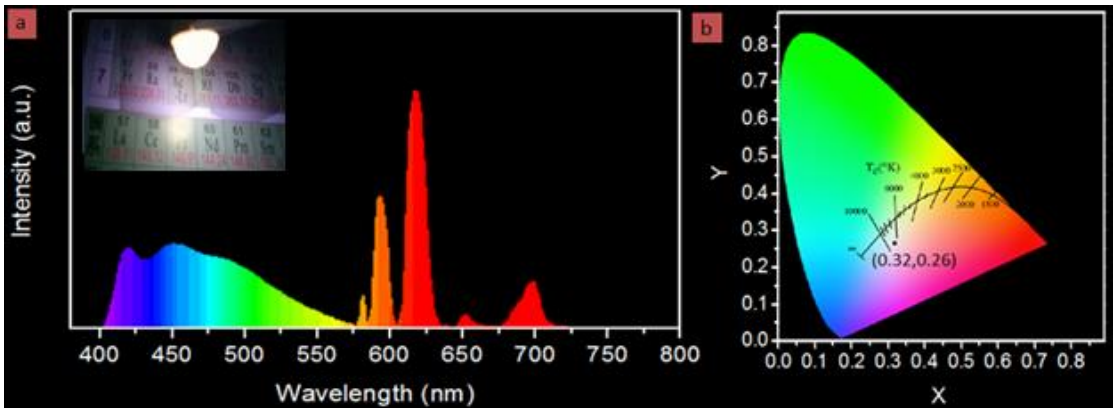

Figure S14. (a) Emission spectrum and **(b)** CIE chromaticity coordinates of the white LED based on $CsPbCl_3$ NCs doped with 2 mol% Ce^{3+} and 8 mol% Eu^{3+} ions. Inset of Figure (a) is the photograph of white LED operated at 3.0 V.

Because the Eu^{3+} ions $CsPbCl_3$ NCs possess stable red emission, and the Ce^{3+} ions $CsPbCl_3$ NCs possess stable blue and green emission, Ce^{3+} and Eu^{3+} ions co-doped $CsPbCl_3$ NCs are constructed to fabricate white LEDs. The LED device exhibits cool white emission (Inset in Figure S14a). Figure S14a presents the emission spectra of the white LED operated at 3.0 V, in which one broad band from 400 to 550 nm contributed by the exciton and intrinsic transition of Ce^{3+} ions, as well as a series peaks from intrinsic transition of Eu^{3+} ions are observed. Those emitting components induce a white light emission with the color coordinate of (0.32, 0.26) (Figure S14b).

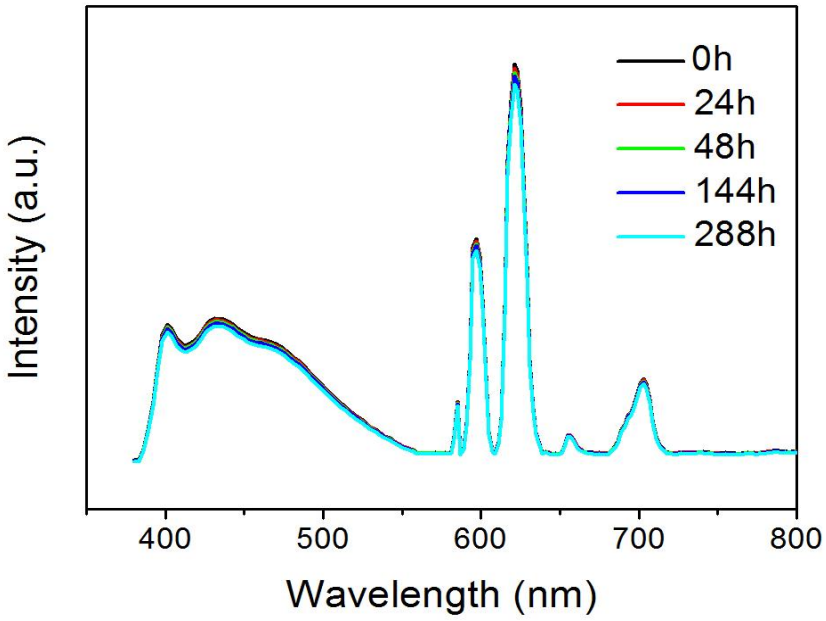

Figure S15. The emission spectra of the white LED device acquired at different working times at the bias of 3.0 V.

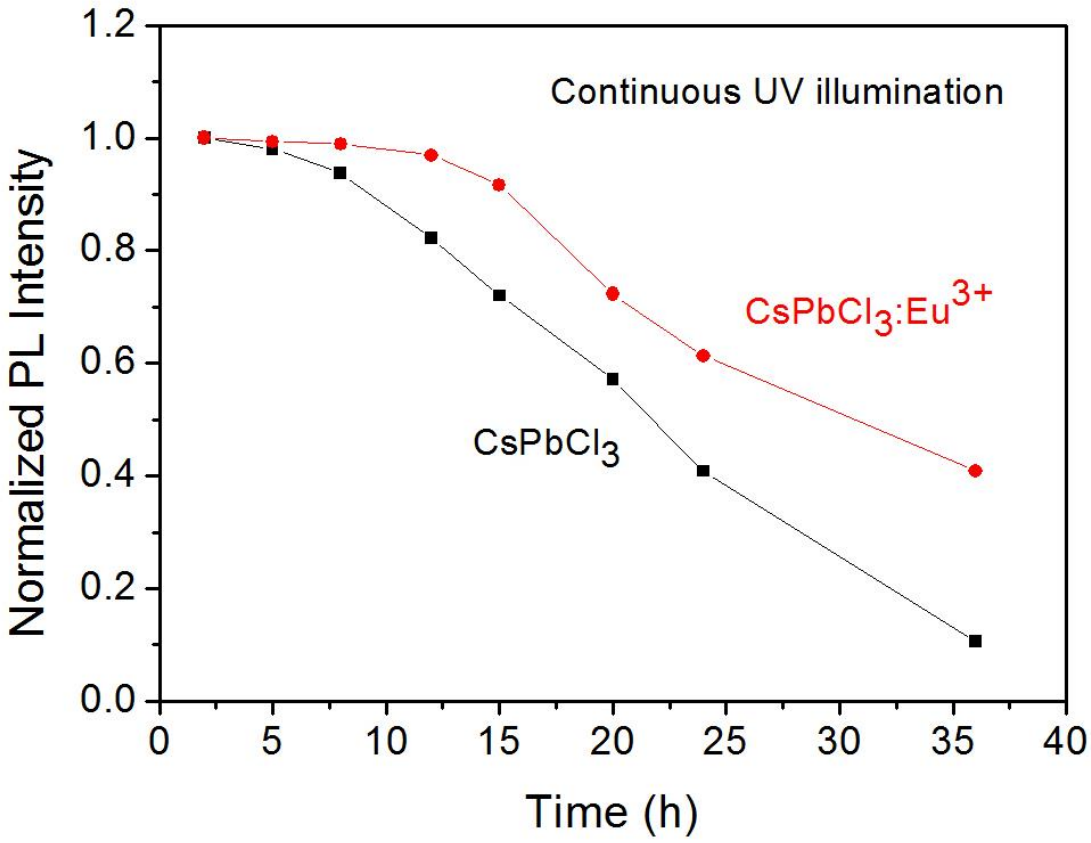

Figure S16. The normalized exciton emission intensity as a function of UV irradiated time for the undoped and (7.8 mol%) Eu^{3+} ions doped $CsPbCl_3$ perovskite NCs.

The power and emission wavelength of UV lamp is 6 W and 365 nm, respectively. Two samples have been detected for 36h. The result shows that the photoluminescence stability of the perovskite NCs improved obviously as introducing of Eu^{3+} ions.

Table S1. Parameters for undoped $CsPbCl_3$ NCs and NCs doped with different lanthanide ions.

	Undoped NCs	NCs doped with different lanthanide ions						
Doping ion	N/A	Ce^{3+}	Sm^{3+}	Eu^{3+}	Tb^{3+}	Dy^{3+}	Er^{3+}	Yb^{3+}
Radius of doping ion (Å)	N/A	1.034	0.964	0.950	0.923	0.908	0.881	0.858
lattice constant (101) (Å)	3.96	3.94	3.93	3.92	3.90	3.89	3.88	3.87
Band gap (eV)	2.87	2.91	2.94	2.98	3.03	3.05	3.08	3.10
Doping concentration (mol%) from ICP characterization	N/A	7.2	7.3	7.9	7.6	7.4	7.8	9.1
Photoluminescence QY for the overall emission band (%)	3.8	24.3	14.1	27.2	31.2	27.6	15.1	142.7

Table S2. Emission decays of respective intrinsic emissions of lanthanide ions in the doped $CsPbCl_3$ NCs.

Lanthanide ion	Monitoring wavelength (nm)	Lifetime τ (μs)
Ce^{3+}	430	$9.7x10^{-3}$
Sm^{3+}	605	600
Eu^{3+}	620	714
Tb^{3+}	550	598
Dy^{3+}	572	583
Er^{3+}	548	654
Yb^{3+}	982	588

Note: lifetimes are acquired by fitting the decay curves from the function of $I(t) = I\exp(-t/\tau)$.

Table S3. Emission decay of excitonic transitions (monitored at 410 nm) for NCs doped with different lanthanide ions.

Lifetime / Sample	τ_1(ns)	a_1	τ_2(ns)	a_2	$\bar{\tau}$(ns)
$CsPbCl_3$	3.6	23%	4.3	77%	4.1
$CsPbCl_3$:Ce	2.7	20%	4.1	80%	3.7
$CsPbCl_3$:Sm	5.2	18%	6.4	82%	6.2
$CsPbCl_3$:Eu	4.9	19%	7.1	81 %	6.7
$CsPbCl_3$:Tb	5.1	17%	7.4	83%	7.1
$CsPbCl_3$:Dy	5.4	26%	7.9	74%	7.6
$CsPbCl_3$:Er	4.6	16%	8.8	84%	8.2
$CsPbCl_3$:Yb	4.4	22%	10.1	78%	9.1

Note: lifetimes are acquired by fitting the decay curves from the function of $I(\mathrm{t}) = I_1 \exp(-t/\tau_1) + I_2 \exp(-t/\tau_2)$; the average lifetimes were got by $\bar{\tau} = \frac{a_1\tau_1^2 + a_2\tau_2^2}{a_1\tau_1 + a_2\tau_2}$.

Table S4. Fitting parameters of normalized transient absorption data for the undoped and Eu^{3+} ions doped $CsPbCl_3$ NCs.

sample	a_1	a_2	a_3	τ_1(ps)	τ_2(ns)	τ_3(ps)
$CsPbCl_3$	0.37±0.03	0.63±0.03	n/a	3.4±0.7	3.5±0.3	n/a
$CsPbCl_3$:7.8%Eu	0.38±0.03	0.42±0.03	0.2±0.03	5.2±1.1	5.6±0.6	113±10

Note: time constants are acquired by fitting the decay curves from the function of $\sum a_i \exp(t/\tau_i)$.

Table S5. Eu/Pb molar ratio used during synthesis measured by ICP-MS from which Eu^{3+} ions per nanocrystal are calculated.

Eu/Pb mol% used in feed solution	Eu^{3+} ion doping concentration (mol%) from ICP characterization	Injection temperature (°C)
50	1.2 ± 0.01	180
50	2.7 ± 0.01	200
50	7.8 ± 0.01	240
50	11.1 ± 0.01	260

Table S6. The lattice constants of Eu^{3+} doped $CsPbCl_3$ NCs with different doping concentrations.

doping concentrations (mol%)	1.2	2.7	7.8	11.1
lattice constant (101) (Å)	3.96	3.95	3.92	3.90

Note: the lattice constants are from XRD patterns of the Eu^{3+} ions doped $CsPbCl_3$ NCs with different doping concentrations.

REFERENCES

1. Xu, P.; Chen, S.; Xiang, H.-J.; Gong, X.-G.; Wei, S.-H. *Chem. Mater.* **2014,** 26, 6068-6072.

2. Yin, W.-J.; Shi, T.; Yan, Y. *Appl. Phys. Lett.* **2014,** 104, 063903.

3. Xiao, Z.; Zhou, Y.; Hosono, H.; Kamiya, T. *Phys. Chem. Chem. phys.* **2015,** 17, 18900-18903.

4. Kang, J.; Wang, L. W. *J. Phys. Chem. Lett.***2017,** 8, 489-493.

5. Blöchl, P. E. *Phys. Rev. B* **1994,** 50, 17953-17979.

6. Shishkin, M.; Kresse, G. *Phys. Rev. B* **2007,** 75, 235102.

7. Lany, S.; Zunger, A. *Phys. Rev. B* **2008,** 78, 235104.